Positron scattering from molecular hydrogen

J. R. Machacek,[1,*] E. K. Anderson,[1] C. Makochekanwa,[1] S. J. Buckman,[1,2] and J. P. Sullivan[1]

[1]*ARC Centre for Antimatter-Matter Studies, Research School of Physics and Engineering, Australian National University, Canberra, 0200 Australia*

[2]*Institute of Mathematical Sciences, University of Malaya, Kuala Lumpur, Malaysia*

(Received 20 May 2013; published 31 October 2013)

We present results for total and partial cross sections for positron scattering from H_2. The total scattering and positronium formation cross sections are reported between 0.5 and 200 eV. Total quasielastic and inelastic scattering cross sections are reported for energies between the positronium formation threshold and 50 eV, with quasielastic differential scattering cross sections reported at 1, 3, 5, 7, and 10 eV. Our results are compared with previous work, both experimental and theoretical, with particular attention paid to the region below the positronium formation threshold, where there are apparent discrepancies in previous work. A discussion of possible reasons for discrepancies between this and previous work is presented, including a focus on known systematic effects in the experimental results.

DOI: 10.1103/PhysRevA.88.042715 PACS number(s): 34.80.Uv, 34.80.Lx, 34.80.Gs, 34.80.Bm

I. INTRODUCTION

Molecular hydrogen is the simplest neutral molecule and it has been extensively studied in a range of lepton collisions, but the results for positron scattering from H_2 are still incomplete. An example of this is the lack of scattering information for rotational excitation, and only limited data for vibrational [1] and electronic excitation [2] processes or even elastic scattering [3]. This is largely due to the historically limited availability of high-resolution positron beams, with the concomitant difficulty in resolving discrete partial cross sections.

It has been 40 years since Coleman *et al.* and Hoffman *et al.* [4,5] published the first low-energy total cross sections for positron-H_2 scattering. Since then, there have been a number of experimental and theoretical results, many of which have been summarized in a recent review [6]. At energies above the positronium formation threshold there is general agreement, when experimental errors are taken into account, in both the magnitude and energy dependence of the total cross section on the experimental side (with the possible exception of the data of Charlton *et al.* [7]), if not for the limited number of theoretical calculations available. Below threshold, this is not the case. In this energy region there are a broad range of reported results, both experimental and theoretical, which are in apparent disagreement with each other, with the recent results of the Trento group [8] noticeably higher than any other calculation or measurement.

Figure 1 shows the state of theoretical and experimental results for the total scattering cross section for positron-H_2 scattering before the present experimental program was undertaken, including a range of theory and experiment [7,9–17]. It does not incorporate our present measurements and the very recent convergent-close-coupling (CCC) theory of Zammit *et al.* [18]. The observed discrepancies in this figure, between both theory and experiment, were a significant motivation for the current study. A notable point, in the case of the previous experimental data, is that each experiment has differing angular acceptance of scattered positrons, with the Trento apparatus having the best discrimination against forward scattered positrons of those experiments presented in Fig. 1. This is the likely source of much of the observed discrepancy, as explained in a previous publication [19].

When a positron with incident energy in the range of 0–200 eV collides with a H_2 molecule, the following scattering processes may occur:

$$
\begin{aligned}
e^+ + H_2(\nu, J) &\rightarrow e^+ + H_2, && \text{elastic,} && (1)\\
&\rightarrow e^+ + H_2(\nu', J'), && \text{rovibrational excitation,} && (2)\\
&\rightarrow H + H, && \text{dissociation,} && (3)\\
&\rightarrow e^+ + H_2^*, && \text{single electronic excitation,} && (4)\\
&\rightarrow e^+ + H_2^{**}, && \text{double electronic excitation} && (5)\\
&\rightarrow e^+ + {H_2}^+ + e^-, && \text{direct ionization,} && (6)\\
&\rightarrow e^+ + 2H^+ + 2e^-, && \text{double ionization} && (7)\\
&\rightarrow Ps + {H_2}^+, && \text{positronium formation} && (8)
\end{aligned}
$$

In the present series of experiments, we have focused on measurements of the grand total, total positronium formation, and total inelastic scattering cross sections. Due to some systematic limitations of the experimental technique, we are unable to

*Present address: Jet Propulsion Laboratory, California Institute of Technology, Pasadena, CA, USA.

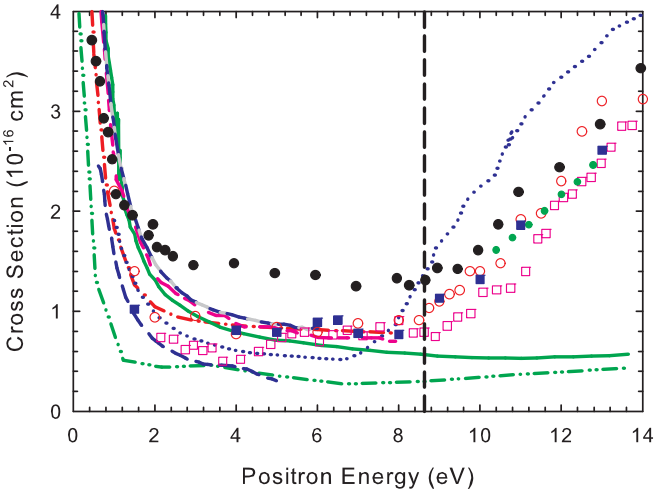

FIG. 1. (Color online) A comparison of the experimental and theoretical results preceding the current results and excluding recent results of Zammit *et al.* [18]. Experimental data: black circles, Zecca *et al.* [8]; open circles, Hoffman *et al.* [5]; open squares, Charlton *et al.* [7]; small circles, Sullivan *et al.* [9]; solid squares, Zhou *et al.* [15]. Theoretical data: dash-dotted line, Gibson *et al.* [16]; solid line, Armour *et al.* [10]; dotted line, Reid *et al.* [17]; long-short line, Arretche *et al.* [11]; long-short line, Mukherjee *et al.* [12]; dash-dot-dotted line, Danby *et al.* [13], dashed line, Gianturco *et al.* [14]. The vertical dashed line indicates the threshold energy for the formation of positronium at 8.643 eV.

discriminate between elastic scattering and vibrational or rotational excitation. However, we have measured quasielastic (i.e., summed over vibrational and rotational excitation) total and angular differential positron scattering up to 50 eV. These results provide absolute scattering cross sections which can be used in models of positron transport, or in detailed comparisons with state-of-the-art quantum scattering calculations.

II. EXPERIMENTAL

The details of the experimental apparatus and the techniques used have been described in detail elsewhere ([20] and references therein), and that detail will not be repeated here. Briefly, positrons from the radioactive decay of ^{22}Na are moderated by a solid neon moderator and loaded into a Surko buffer gas trap. The trap produces a pulsed positron beam with a repetition rate of ∼100 Hz and an energy width of 60 meV, which is radially confined in a 500-G magnetic field. These positrons then pass through a scattering cell 100 mm long which contains the target gas, H_2 for the present work. The target gas pressure is monitored with a capacitance manometer (MKS Baratron model 690A01TRA). Due to the magnetic confining field, the positron motion can be separated into components parallel and perpendicular to the field lines. The parallel energy corresponds to the motion in the direction of the magnetic field lines, and parallel energy loss of the positrons is determined after their passage through the gas cell using a retarding potential analyzer (RPA). This allows the measurement of the total scattering and positronium formation cross sections, and the contribution from the elastic and inelastic scattering channels is able to be separately measured by adjusting the magnetic field in the RPA section, as described previously [21].

TABLE I. Missing forward angles for the experiments presented in this work, and estimated corrections required to the grand total cross section. See text for details.

E (eV)	θ_C (deg)	Missing (%)
1	23	16
3	13	12
5	10	9
7	8	6

A. Grand total scattering cross section

The grand total scattering cross section (GTCS) was determined using the Beer-Lambert law,

$$\sigma_{\mathrm{GTCS}} = -\frac{1}{nl}\ln\left(\frac{I_T}{I_o}\right), \tag{1}$$

where I_o is the intensity of the incident beam, I_T is the intensity of the unscattered portion of the beam after transmission through the gas cell, and n and l are the gas density and the length of the scattering cell respectively. The measurement of n and l provide the absolute normalization of the measurements, and the errors associated with these measurements are relatively small in this case, typically less than 1%. The main source of error comes from the statistical quality of the data, and all errors provided for the measurements presented in this paper are absolute. Due to the magnetic confinement, the energy resolution of the positron beam is related to the angular resolution, and our finite-energy resolution becomes the ultimate limit to the angular resolution of the measurement. Some portion of the forward scattered positrons are not distinguishable from the unscattered beam, and thus our estimates of the total scattering cross section always represent a lower limit of the true value—this is true for all experimental measurements using a transmission technique. A discussion of this issue, and a method for estimating its correction, has been provided in a previous paper [19]. The minimum angle of scattering that we were able to resolve (θ_C) for these measurements is given in Table I, along with the estimated missing percentage of the total cross section, based on the theoretical results of Reid *et al.* [17]. The choice of theoretical results used to determine the missing percentage was based on the agreement in the angular dependence rather than the magnitude of the cross section, and is discussed further below.

B. Positronium formation cross section

As discussed previously [22], the positronium (Ps) formation cross section can be determined by measuring the number of positrons which are lost upon transmission through the gas cell, when the RPA is set to transmit all positrons which have lost any energy (as they are no longer magnetically confined, the positronium atoms are lost from the beam). By comparing the intensity of the positron beam below the positronium formation threshold to that at the energy of interest, it is possible to determine the proportion of positrons undergoing the positronium formation process. If the number of positrons

which undergo positronium formation is given by I_{Ps}, then the cross section can then be calculated by

$$\sigma_{Ps} = \frac{I_{Ps}}{I_o - I_T}\sigma_{\mathrm{GTCS}}. \tag{2}$$

with I_o and I_T defined as previously.

C. Total elastic and inelastic scattering cross sections

The total elastic and total inelastic cross sections are determined from the parallel energy loss spectrum when a magnetic field difference is applied between the scattering cell and RPA, as has been described previously [21,23]. Briefly, the magnetic field at the RPA is reduced compared to the field at the scattering cell. This effectively reduces the parallel energy spread induced by any angular scattering, allowing processes with different total energy loss to be separated [21,23]. In a method similar to that described for positronium formation, the relative proportion of positrons undergoing elastic and inelastic collisions can be measured, and hence the cross section determined. It should be noted that due to the limitations of the practical application of the magnetic field ratio, combined with the energy resolution of the positron beam, rotational and vibrational excitation are not able to be distinguished from elastic scattering in this case, so that the quasielastic cross sections presented here are, in fact, summed over these processes.

D. Differential scattering cross section

The elastic differential cross section was determined using

$$\sigma_{\mathrm{DCS}} = \frac{\sqrt{E_{||}E}}{\pi n l I_o}\left(\frac{dI_C(E)}{dE_{||}}\right), \tag{3}$$

and the derivation of this expression has been discussed previously [21]. Briefly, for a given scattering energy (E) the parallel energy loss was measured with the RPA [$I_C(E_{||})$]. The derivative of $I_C(E_{||})$ is proportional to the differential scattering cross section, with the absolute normalization determined from the beam intensity (I_o), gas number density (n), the length of the scattering cell (l), the scattering energy (E), and the parallel energy ($E_{||}$). Positrons scattered through angles of greater than 90 deg are reflected at the trap and pass back through the gas cell. With a low probability of scattering (kept to less than 10% in the measurements presented here), it can be assumed that these positrons transit the gas cell again without scattering, and so the measured differential cross section is "folded" around 90 deg, so that the measurement is actually the sum of scattering at θ and $(180 - \theta)$ deg. Again, this technique results in absolute normalization of the cross-section values, and absolute errors are quoted for the data. At energies above the first inelastic threshold, the magnetic field ratio technique described above is used to separate elastic from inelastic scattering.

III. RESULTS AND DISCUSSION

A. Total cross-section comparison

Our total scattering results below 10 eV are shown in Fig. 2, with tabulated data in Table II. In this figure we compare our experimental results with selected previous work, including

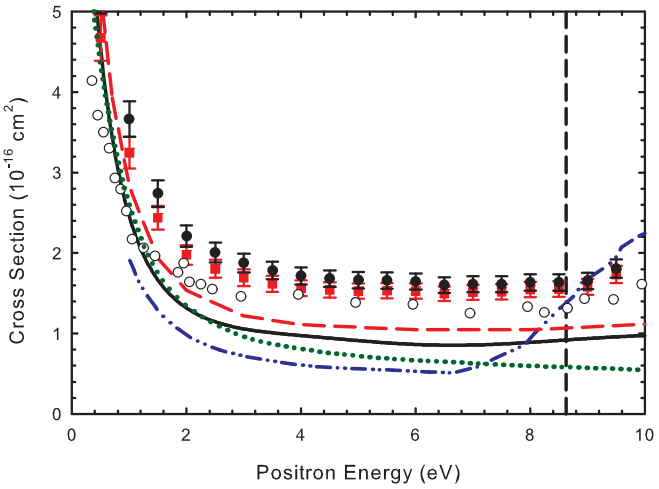

FIG. 2. (Color online) Experimental and theoretical results for the total cross section below the ionization threshold. Experimental results: solid squares, current results; solid black circles, angular correction applied, see text; open circles, Trento results [8]. Theoretical results: dash-dot-dotted line, Reid *et al.* [17]; black solid line, Zhang *et al.* [24]; dotted line, Tenfen [25]; and dashed line, Zammit *et al.* [18]. The vertical dashed line indicated the positronium formation threshold.

the experimental data of the Trento group [8], the theoretical results of Reid *et al.* [17], along with the most recent results of Zhang *et al.* [24], Tenfen [25], and Zammit *et al.* [18]. The total cross section with estimated corrections for our missing angular range is also shown, using the calculations of Reid *et al.*, as discussed previously. Our results appear larger in magnitude than all previous work, even that of the Trento group, which was far larger in magnitude than all previous experimental data (see Fig. 1). However, it must be noted that other experimental results in Fig. 1 have far worse angular resolution; for instance, Hoffman *et al.* [5] reported a minimum angle of 25 deg at 5 eV, Charlton *et al.* [7] reported minimum angle of 20 deg, and Zhou *et al.* [15] reported a minimum angle of 24 deg at 20 eV. Our angular resolution for these measurements was considerably better than all of these (see Table I), and we believe this accounts for most of the apparent differences in the results. The comparison with the Trento data shown in the figure is also consistent with comparisons of recent measurements from our two groups, although they claim a somewhat better angular resolution than these experiments [26].

In this energy range, the experimental data lies higher in magnitude than all the theoretical calculations shown in Fig. 2, as well as the other theories shown in Fig. 1. The reasons for this are less clear, as the calculations have none of the angular resolution difficulties that are seen in the case of experiment. For the most part the theories represent the relative shape of the cross section reasonably well, while underestimating the magnitude. In the case of Reid *et al.*, an increase in the cross section at energies above 7 eV is not seen in any of the other calculations or in the experimental data. One obvious consideration in the comparison with theory is that the calculations do not take into account vibrational and rotational excitation, with all calculations being performed

TABLE II. Grand total scattering and positronium formation cross section (10^{-16} cm^2).

Energy (eV)	σ_{GTCS}	Δ_{GTCS}	σ_{Ps}	Δ_{Ps}
0.50	4.67	0.28		
1.00	3.25	0.20		
1.50	2.44	0.15		
2.00	1.98	0.12		
2.50	1.80	0.11		
3.00	1.69	0.10		
3.50	1.62	0.10		
4.00	1.56	0.10		
4.50	1.54	0.10		
5.00	1.53	0.09		
5.50	1.53	0.09		
6.00	1.53	0.09		
6.50	1.49	0.09		
7.00	1.51	0.09		
7.50	1.52	0.09		
8.00	1.55	0.10		
8.50	1.55	0.10		
9.00	1.58	0.10		
10.00	1.56	0.11	0.51	0.12
15.00	3.67	0.14	2.12	0.14
20.00	4.94	0.15	2.78	0.15
25.00	5.10	0.15	2.54	0.15
30.00	4.83	0.14	2.06	0.14
35.00	4.67	0.15	1.65	0.14
40.00	4.60	0.15	1.51	0.13
45.00	4.37	0.14	1.32	0.13
50.00	4.22	0.14	1.22	0.13
55.00	3.97	0.14	1.11	0.13
60.00	3.89	0.14	0.94	0.13
65.00	3.79	0.14	0.76	0.13
70.00	3.68	0.13	0.66	0.13
75.00	3.49	0.14	0.43	0.13
80.00	3.26	0.13	0.33	0.12
85.00	3.15	0.13	0.26	0.12
90.00	3.12	0.13	0.45	0.13
95.00	3.17	0.13	0.47	0.12
100.00	2.90	0.13	0.23	0.12
105.00	2.85	0.13	0.40	0.12
110.00	2.88	0.13	0.35	0.12
115.00	2.67	0.13	0.22	0.13
120.00	2.66	0.13	0.32	0.13
125.00	2.52	0.12	0.25	0.12
130.00	2.66	0.13	0.43	0.13
135.00	2.32	0.12	0.08	0.12
140.00	2.50	0.12	0.36	0.12
145.00	2.35	0.12	0.30	0.13
150.00	2.11	0.12	0.08	0.12
155.00	2.14	0.12		
160.00	2.34	0.12		
165.00	2.11	0.12		
170.00	2.09	0.12		
175.00	1.93	0.12		
180.00	1.86	0.11		
185.00	1.97	0.12		
190.00	1.88	0.12		
195.00	1.97	0.12		

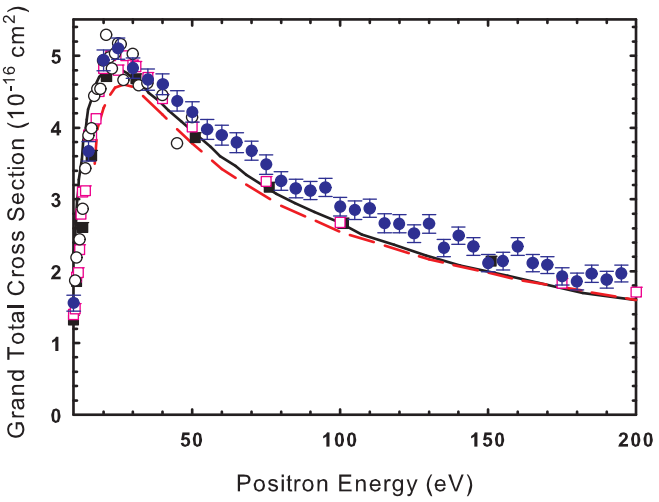

FIG. 3. (Color online) Comparison of results for the grand total cross section (GTCS) from 10 up to 200 eV. Experimental results: filled circles, current results; open black circles, Zecca *et al.* [8]; open squares, Hoffman *et al.* [5]; filled black squares, Zhou *et al.* [15]. Theoretical results: solid black line, results from Reid *et al.* [17]; dashed line, results from Zammit *et al.* [18].

with a fixed internuclear distance of 1.4 a_0. Both vibrational and rotational excitation are included in the experimental data and it may be that including these processes will improve the agreement. However, given the magnitude of the vibrational excitation measured by Sullivan *et al.* and reasonable estimates of the rotational excitation, it is unlikely that this can account for all of the difference between experiment and theory in this case.

The comparison of the current results with previous work from 10 eV up to energies of 200 eV is shown in Fig. 3. At energies above the positronium formation threshold, the various experimental results converge, with no difference within the stated errors of the measurements. This is consistent with previous observations that differences in angular resolution become less important as the scattering energy increases. The peak of the total cross section at around 25 eV corresponds to the maximum of the positronium formation cross section (presented below). The comparison between experiment and theory is also very good in this energy range, with the calculations lying perhaps a little lower than the measurements at energies above 50 eV. The underestimation of the most recent theoretical results of Zammit *et al.* [18] below 30 eV will likely be resolved as understanding of how the positronium formation channel couples to the elastic scattering channel, and in particular the role of virtual positronium states, is improved.

B. Positronium formation

The current measurements for the positronium formation cross section are shown in Fig. 4, along with previous experimental and theoretical efforts [15,27–30]. The tabulated results are also shown in Table II. The results show a typical shape for this cross section, rising to a peak at ∼25 eV and then falling away, as the ionization channel opens, to effectively zero at around 150 eV. The agreement with previous experimental

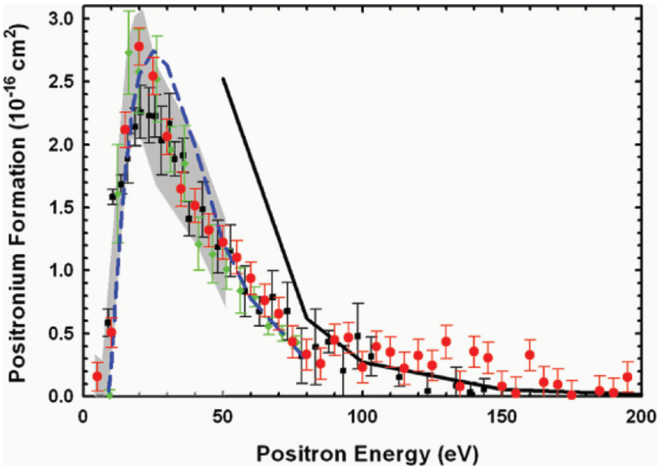

FIG. 4. (Color online) Comparison of the positronium (Ps) formation cross section up to 200 eV. Experimental results: filled circles, current data; black squares, Fromme *et al*. [27]; filled gray area, experimental results from Zhou *et al*. [15]; diamonds, Fornari *et al*. [28]. Theoretical results: solid black line, first-order Born approximation (FBA) from Biswas *et al*. [29]; dashed line, Ps(1*s*) CS calculations of Biswas *et al*. [30].

results is excellent. Theoretical results for the positronium formation cross section are included in Fig. 4. We see general agreement with one of the coupled-state calculations of Biswas *et al*. [30] at energies below 80 eV. Above 50 eV, a simplified second-order perturbative Born series was used in an earlier calculation by Biswas *et al*. [29], but theory and experiment do not converge until approximately 70 eV.

C. Differential cross section

The quasielastic (summed over rotations and vibrations) differential cross section (DCS) was measured at energies of 1, 3, 7, and 10 eV, with the data presented in Table III. We also note here that there has been one previous measurement of the elastic differential cross section for positron scattering from molecular hydrogen by Sullivan *et al*. [3], although this was at 0.5 eV, and thus below the range of energies considered in this work. Figure 5 compares the current experimental results with those from available theory [16–18,24,25,31]. Comparison of the experimental and theoretical results show general agreement in angular dependence but, as was the case with the total cross sections, the magnitude is significantly different, with the experimental results being larger and more forward peaked in all cases. The results of Reid *et al*. [17] are in best agreement with the experimental results in terms of the angular dependence, but the magnitude is different by a factor of almost three, and this factor is nearly constant over the range of energies covered by the experimental results. On the basis of the agreement in the shape of the DCS, these calculations were used to correct the total scattering cross section for the missing angular contribution. This was done by calculating the missing percentage of the TCS corresponding to the calculation, using the angular discrimination of the experiment (see Table I). This percentage correction is then applied to the experimental measurements to estimate the true total cross section. The recent CCC results from Zammit *et al*. [18] obtain better agreement in magnitude across the experimental results, which is again represented in the comparison at the total cross section level. Other theories have varying degrees of agreement in terms of the shape of the DCS but are much smaller in magnitude that the experimental data. One major difference between the experiments in this case and the theoretical approaches is the inclusion of vibrational and rotational excitation in the experimental data. This may account for some of the difference in observed magnitude, although previous measurements of the vibrational total cross section [1] suggest that this is at most only 10% of the total scattering in this energy range, and thus not enough to make up for all of the differences in theory and experiment.

TABLE III. Folded differential scattering cross section (10^{-16} cm^2 sr^{-1}) at 1, 3, 7, and 10 eV.

Angle (deg)	σ_{DCS} (1 eV)	Δ_{DCS}	σ_{DCS} (3 eV)	Δ_{DCS}	σ_{DCS} (7 eV)	Δ_{DCS}	σ_{DCS} (10 eV)	Δ_{DCS}
12.50							2.07	0.08
17.50					1.31	0.05	1.38	0.06
22.50	1.30	0.07	1.01	0.04	0.94	0.04	0.82	0.05
27.50	1.34	0.06	0.89	0.03	0.61	0.03	0.62	0.04
32.50	0.98	0.05	0.70	0.03	0.46	0.03	0.39	0.03
37.50	0.92	0.05	0.49	0.02	0.33	0.02	0.21	0.03
42.50	0.79	0.04	0.34	0.02	0.23	0.02	0.22	0.03
47.50	0.80	0.04	0.29	0.02	0.15	0.02	0.11	0.02
52.50	0.65	0.04	0.23	0.02	0.14	0.02	0.08	0.02
57.50	0.53	0.03	0.17	0.02	0.09	0.02	0.08	0.02
62.50	0.46	0.03	0.12	0.02	0.09	0.02	0.09	0.02
67.50	0.38	0.03	0.07	0.02	0.09	0.02	0.07	0.02
72.50	0.30	0.03	0.03	0.02	0.03	0.02	0.11	0.02
77.50	0.24	0.03	0.05	0.02	0.07	0.02	0.08	0.02
82.00			0.01	0.02	0.05	0.02	0.07	0.02

D. Quasielastic total cross section

Our results for the quasielastic total scattering cross section above 8.2 eV are shown in Fig. 6, with tabulated data in Table IV. In the case of this measurement, compared to the total cross-section measurements presented in Sec. III A, more of the forward angle distribution is missed. This is due to the use of the magnetic field ratio technique used to separate elastic from inelastic scattering. As a result, the measured elastic scattering does not merge smoothly with the total cross section below the first inelastic threshold, as can be seen in Fig. 6. Nonetheless, we can make a comparison with the calculation of the elastic cross section by Zammit *et al*. [18] above the positronium formation threshold. Within the error of the experimental measurement, agreement with the calculation is good, although the effect of the missing forward angles is likely to make the comparison less favorable. On the other hand, the fact that the measurement also includes contributions from vibrational and rotational excitation would tend to raise the value of the cross section, and these effects will tend to cancel each other. It appears that the energy dependence of the cross section is a little different between theory and experiment, with a steeper decline as energy increases in the theory, although given the size of the error bars it is difficult to be conclusive.

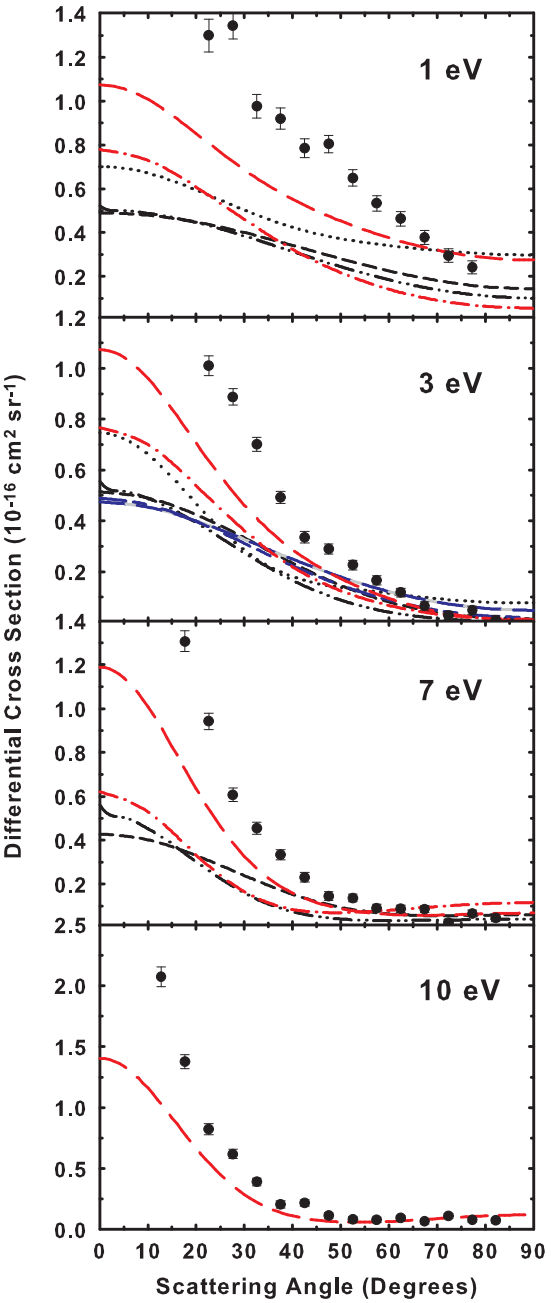

FIG. 5. (Color online) Comparison of experimental and theoretical results for elastic differential cross section at various energies. Solid circles, current experimental results. Theoretical results near 1 eV: black short-dashed line, Lino *et al.* (1.36 eV) [31]; black dash-dot-dotted line, Reid *et al.* (1.36 eV) [17]; black dotted line, Zhou *et al.* [24] (1 eV); dash-dotted line Gibson *et al.* [16] (1.36 eV); long-dashed line, Zammit *et al.* (1 eV) [18]. Theoretical results near 3 eV: black short-dashed line, Lino *et al.* (3.5 eV) [31]; black dash-dot-dotted line, Reid *et al.* (3.5 eV) [17]; black dotted line, Zhou *et al.* (3 eV) [24]; dash-dotted line, Gibson *et al.* (2.72 eV) [16]; long-dashed line, Zammit *et al.* (3 eV) [18]; long-dashed and short-dashed (2.72 eV) and long-short (3.5 eV) lines, Tenfen *et al.* [25]. Theoretical results near 7 eV: black short-dashed line, Lino *et al.* (6.9 eV) [31]; black dash-dot-dotted line, Reid *et al.* (6.9 eV) [17]; dash-dotted line, Gibson *et al.* (6.8 eV) [16]; long-dashed line, Zammit *et al.* (7 eV) [18]. Theoretical results at 10 eV: long-dashed line, Zammit *et al.* [18].

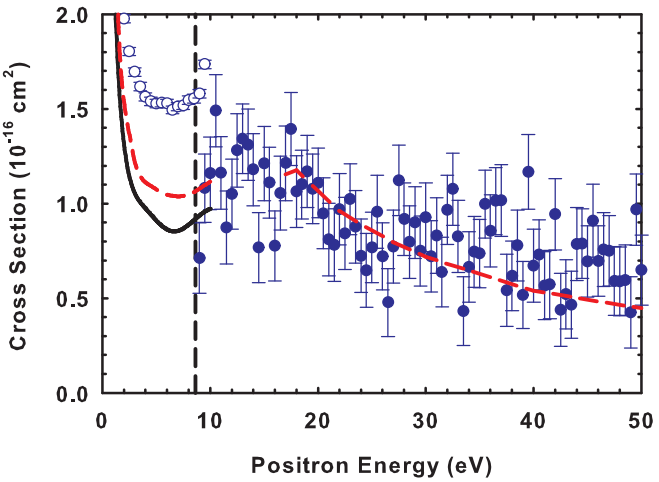

FIG. 6. (Color online) Comparison of total elastic cross section to previous theoretical results. Open circles, current experimental results for grand total cross section; solid circles, current results for the total elastic cross section. Theoretical results for the total elastic scattering cross section: solid black line, Zhang *et al.* [24]; dashed line, Zammit *et al.* [18].

E. Total inelastic cross section

Figure 7 shows the measured total inelastic cross section, which is the sum of all inelastic scattering channels (for example, electronic excitation, single and double ionization, but excluding rotational and vibrational excitation and positronium formation), up to 50 eV. The data are also given in Table IV. We compare this data with previous theoretical and experimental results below 50 eV. Sullivan *et al.* [1] measured the cross section for the $B^1\Sigma$ electronic excitation up to 30 eV, and this is also shown in the figure. The theoretical ionization

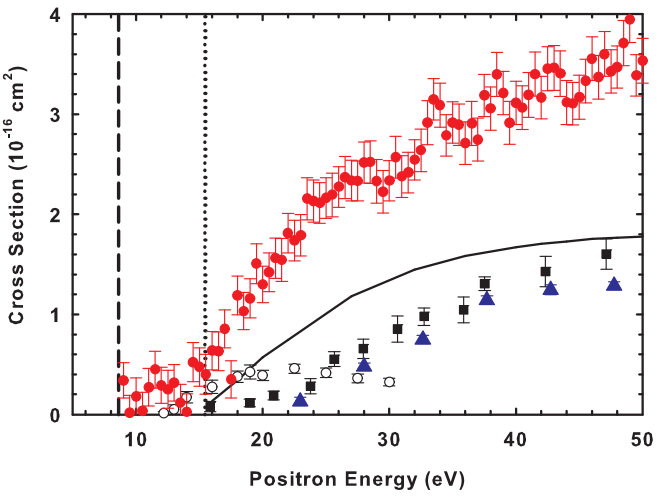

FIG. 7. (Color online) Comparison of results for the excitation of inelastic channels in positron-H_2 scattering. Solid circles, current experimental results for the total inelastic cross section; open circles, results for the excitation of the $B^1\Sigma$ state by Sullivan *et al.* [1]; black squares, results for direct ionization of H_2 by Fromme *et al.* [27]; triangles, direct ionization measurements of Moxom *et al.* [33]; black line, theoretical results for single ionization by Campeanu *et al.* [32]. The vertical dashed line indicates the positronium formation threshold and the vertical dotted line indicates the ionization threshold.

TABLE IV. Elastic and total inelastic (without Ps) scattering cross sections (10^{-16} cm^2 sr^{-1}).

Energy (eV)	σ_{Elastic}	Δ_{Elastic}	$\sigma_{\text{Inelastic-Ps}}$	$\Delta_{\text{Inelastic-Ps}}$	Energy (eV)	σ_{Elastic}	Δ_{Elastic}	$\sigma_{\text{Inelastic-Ps}}$	$\Delta_{\text{Inelastic-Ps}}$
9.00	0.71	0.19	0.34	0.17	30.00	0.93	0.18	2.29	0.20
9.50	1.08	0.18	0.02	0.17	30.50	0.72	0.19	2.52	0.20
10.00	1.16	0.19	0.18	0.18	31.00	0.83	0.20	2.33	0.20
10.50	1.49	0.19	0.04	0.18	31.50	0.64	0.18	2.37	0.20
11.00	1.16	0.19	0.27	0.18	32.00	0.97	0.18	2.50	0.20
11.50	0.87	0.19	0.45	0.18	32.50	1.08	0.19	2.59	0.21
12.00	1.05	0.19	0.29	0.18	33.00	0.83	0.19	2.86	0.22
12.50	1.28	0.19	0.25	0.19	33.50	0.43	0.18	3.09	0.20
13.00	1.34	0.18	0.32	0.18	34.00	0.67	0.19	3.03	0.21
13.50	1.31	0.19	0.12	0.18	34.50	0.75	0.19	2.74	0.20
14.00	1.18	0.19	0.03	0.18	35.00	0.74	0.18	2.86	0.20
14.50	0.77	0.19	0.52	0.19	35.50	1.00	0.18	2.84	0.20
15.00	1.21	0.20	0.47	0.19	36.00	0.86	0.19	2.66	0.21
15.50	1.11	0.19	0.40	0.20	36.50	1.01	0.18	2.86	0.22
16.00	0.78	0.18	0.63	0.19	37.00	1.02	0.19	2.70	0.21
16.50	1.06	0.20	0.63	0.19	37.50	0.54	0.19	3.13	0.21
17.00	1.21	0.20	0.84	0.19	38.00	0.62	0.18	3.00	0.21
17.50	1.39	0.19	0.35	0.18	38.50	0.78	0.19	3.34	0.22
18.00	1.06	0.19	1.17	0.19	39.00	0.52	0.18	3.15	0.21
18.50	1.10	0.18	1.02	0.18	39.50	1.17	0.20	2.86	0.21
19.00	1.17	0.19	1.14	0.19	40.00	0.67	0.19	3.06	0.21
19.50	1.08	0.18	1.48	0.20	40.50	0.73	0.19	3.01	0.22
20.00	1.11	0.18	1.28	0.18	41.00	0.57	0.18	3.13	0.22
20.50	0.95	0.19	1.40	0.19	41.50	0.57	0.18	3.34	0.22
21.00	0.81	0.19	1.53	0.20	42.00	0.94	0.19	3.11	0.21
21.50	0.78	0.19	1.52	0.21	42.50	0.44	0.19	3.39	0.22
22.00	0.97	0.19	1.78	0.19	43.00	0.52	0.18	3.40	0.22
22.50	0.84	0.19	1.71	0.20	43.50	0.47	0.18	3.35	0.22
23.00	1.02	0.19	1.76	0.20	44.00	0.79	0.19	3.06	0.21
23.50	0.88	0.19	2.11	0.21	44.50	0.79	0.18	3.05	0.21
24.00	0.72	0.19	2.09	0.21	45.00	0.69	0.19	3.12	0.22
24.50	0.65	0.20	2.07	0.20	45.50	0.91	0.19	3.27	0.21
25.00	0.77	0.19	2.12	0.20	46.00	0.70	0.19	3.49	0.22
25.50	0.96	0.19	2.15	0.21	46.50	0.76	0.19	3.31	0.21
26.00	0.72	0.18	2.23	0.20	47.00	0.75	0.19	3.54	0.22
26.50	0.48	0.18	2.32	0.21	47.50	0.59	0.18	3.37	0.21
27.00	0.77	0.19	2.29	0.20	48.00	0.59	0.18	3.41	0.21
27.50	1.12	0.19	2.29	0.19	48.50	0.60	0.19	3.65	0.22
28.00	0.92	0.19	2.47	0.20	49.00	0.43	0.19	3.88	0.22
28.50	0.80	0.19	2.47	0.21	49.50	0.97	0.19	3.33	0.20
29.00	0.90	0.19	2.29	0.21	50.00	0.65	0.18	3.47	0.22
29.50	0.75	0.18	2.18	0.21					

results of Campeanu *et al*. [32], along with the experimental results of Fromme *et al*. [27] and Moxom *et al*. [33], for the same process are also shown for a general comparison. The current results are a sum of all inelastic scattering channels and should be larger than any single partial cross section, which is consistent with what can be observed in Fig. 7. However, the magnitude of the total inelastic cross section presented here is substantially larger than any of the other results, even at 50 eV where it might be expected that ionization is the dominant inelastic process. Given fair agreement between the two experiments and the theory for this process at 50 eV, it may be possible that a significant part of this total inelastic cross section arises from electronic excitations (other than the $B^1\Sigma$ state) or even fragmentation. Further studies of the relevant partial cross sections would be useful to try and resolve this apparent discrepancy.

IV. CONCLUSION

We have reported measurements of a number of total and partial cross sections for positron scattering from H_2. Comparison between the present experiment and the other recently published experimental data shows excellent agreement, with observed differences largely explained by a consideration of the differences in forward angle discrimination. The available theoretical results for the total cross section, however, are significantly different in magnitude at low energies to the experimental data. Part of this difference is due to the exclusion

of vibrational and rotational scattering from the calculations, although this is unlikely to account for all of the differences. The measured positronium formation cross section is in good agreement with previous work, including one of the calculations reported by Biswas *et al.* [30]. We have also reported the total inelastic scattering cross section, which appears to indicate some discrepancies when considering previous work on total inelastic measurements but may be explained by the fact that unmeasured (or calculated) processes such as electronic excitation have a larger magnitude than may be initially assumed. Given the discrepancies observed, there is clearly scope for further detailed studies of positron scattering from molecular hydrogen, particularly as this represents the simplest molecular target readily available for comparison between experiment and theory. Understanding and benchmarking of simple systems such as this is crucial for further developing a detailed understanding of low-energy positron scattering.

ACKNOWLEDGMENTS

Funding for this work was provided by the Australia Research Council (ARC) through its Centre of Excellence Program. The authors also thank Steve Battisson and Ross Tranter for the excellent technical support provided during the course of this work.

[1] J. P. Sullivan, S. J. Gilbert, and C. M. Surko, Phys. Rev. Lett. **86**, 1494 (2001).
[2] J. P. Sullivan, J. P. Marler, S. J. Gilbert, S. J. Buckman, and C. M. Surko, Phys. Rev. Lett. **87**, 073201 (2001).
[3] J. P. Sullivan, S. Gilbert, J. P. Marler, L. D. Barnes, S. J. Buckman, and C. Surko, Nucl. Instr. Meth. B **192**, 3 (2002).
[4] P. G. Coleman, T. C. Griffith, and G. R. Heyland, Appl. Phys. **4**, 89 (1974).
[5] K. R. Hoffman, M. S. Dababneh, Y.-F. Hsieh, W. E. Kauppila, V. Pol, J. H. Smart, and T. S. Stein, Phys. Rev. A **25**, 1393 (1982).
[6] C. M. Surko, G. F. Gribakin, and S. J. Buckman, J. Phys. B **38**, R57 (2005).
[7] M. Charlton, T. C. Griffith, G. R. Heyland, and G. L. Wright, J. Phys. B **16**, 323 (1983).
[8] A. Zecca, L. Chiari, A. Sarkar, K. L. Nixon, and M. J. Brunger, Phys. Rev. A **80**, 032702 (2009).
[9] J. P. Sullivan, S. J. Gilbert, S. J. Buckman, and C. M. Surko, J. Phys. B **34**, L467 (2001).
[10] E. A. G. Armour, D. J. Baker, and M. Plummer, J. Phys. B **23**, 3057 (1990).
[11] F. Arretche, R. F. da Costa, S. d. A. Sanchez, A. N. S. Hisi, E. M. de Oliveira, M. T. do N. Varella, and M. A. P. Lima, Nucl. Instr. Meth. B **247**, 13 (2006).
[12] T. Mukherjee and N. K. Sarkar, J. Phys. B **41**, 125201 (2008).
[13] G. Danby and J. Tennyson, J. Phys. B **23**, 1005 (1990).
[14] F. A. Gianturco, P. Paioletti, and J. A. Rodriguez-Ruiz, Z. Phys. D **36**, 51 (1996).
[15] S. Zhou, H. Li, W. E. Kauppila, C. K. Kwan, and T. S. Stein, Phys. Rev. A **55**, 361 (1997).
[16] T. L. Gibson, J. Phys. B **25**, 1321 (1992).
[17] D. D. Reid, W. B. Klann, and J. M. Wadehra, Phys. Rev. A **70**, 062714 (2004).
[18] M. C. Zammit, D. V. Fursa, and I. Bray, Phys. Rev. A **87**, 020701 (2013).
[19] J. P. Sullivan, C. Makochekanwa, A. Jones, P. Caradonna, D. S. Slaughter, J. Machacek, R. P. McEachran, D. W. Mueller, and S. J. Buckman, J. Phys. B **44**, 035201 (2011).
[20] J. P. Sullivan, A. Jones, P. Caradonna, C. Makochekanwa, and S. J. Buckman, Rev. Sci. Instrum. **79**, 113105 (2008).
[21] J. P. Sullivan, S. J. Gilbert, J. P. Marler, R. G. Greaves, S. J. Buckman, and C. M. Surko, Phys. Rev. A **66**, 042708 (2002).
[22] A. C. L. Jones, P. Caradonna, C. Makochekanwa, D. S. Slaughter, R. P. McEachran, J. R. Machacek, J. P. Sullivan, and S. J. Buckman, Phys. Rev. Lett. **105**, 073201 (2010).
[23] S. J. Gilbert, R. G. Greaves, and C. M. Surko, Phys. Rev. Lett. **82**, 5032 (1999).
[24] R. Zhang, K. L. Baluja, J. Franz, and J. Tennyson, J. Phys. B **44**, 35203 (2011).
[25] W. Tenfen, K. T. Mazon, S. E. Michelin, and F. Arretche, Phys. Rev. A **86**, 042706 (2012).
[26] A. Zecca, L. Chiari, A. Sarkar, and M. J. Brunger, New J. Phys. **13**, 115001 (2011).
[27] D. Fromme, G. Kruse, W. Raith, and G. Sinapius, J. Phys. B **21**, L261 (1988).
[28] L. S. Fornari, L. M. Diana, and P. G. Coleman, Phys. Rev. Lett. **51**, 2276 (1983).
[29] P. K. Biswas and A. S. Ghosh, J. Phys. B **30**, 983 (1997).
[30] P. K. Biswas, J. S. E. Germano, and T. Frederico, J. Phys. B **35**, L409 (2002).
[31] J. L. S. Lino, J. S. E. Germano, E. P. da Silva, and M. A. P. Lima, Phys. Rev. A **58**, 3502 (1998).
[32] R. I. Campeanu, J. W. Darewych, and A. D. Stauffer, J. Phys. B **30**, 5033 (1997).
[33] J. Moxom, G. Laricchia, and M. Charlton, J. Phys. B **28**, 1331 (1995).